

# UC San Diego

## UC San Diego Previously Published Works

### Title

Systematic Gene-to-Phenotype Arrays: A High-Throughput Technique for Molecular Phenotyping.

### Permalink

<https://escholarship.org/uc/item/9tk62492>

### Journal

Molecular cell, 69(2)

### ISSN

1097-2765

### Authors

Jaeger, Philipp A  
Ornelas, Lilia  
McElfresh, Cameron  
et al.

### Publication Date

2018

### DOI

10.1016/j.molcel.2017.12.016

Peer reviewed



Published in final edited form as:

*Mol Cell*. 2018 January 18; 69(2): 321–333.e3. doi:10.1016/j.molcel.2017.12.016.

## Systematic Gene-to-Phenotype Arrays: A High-Throughput Technique for Molecular Phenotyping

Philipp A. Jaeger<sup>a,b,#,\*</sup>, Lilia Ornelas<sup>c,#</sup>, Cameron McElfresh<sup>d</sup>, Lily R. Wong<sup>e</sup>, Randolph Y. Hampton<sup>c,\*</sup>, and Trey Ideker<sup>a,\*</sup>

<sup>a</sup>Department of Medicine, University of California, San Diego, La Jolla, CA 92093, USA

<sup>b</sup>Biocipher<sub>x</sub> Inc., San Diego, CA 92121, USA

<sup>c</sup>Section of Cell and Developmental Biology, Division of Biological Sciences, University of California, San Diego, La Jolla, CA 92093, USA

<sup>d</sup>Nanoengineering Program, University of California San Diego, La Jolla, California, CA 92093, USA

<sup>e</sup>Bioengineering Program, University of California San Diego, La Jolla, California, CA 92093, USA

### SUMMARY

We have developed a highly parallel strategy, Systematic Gene-to-Phenotype Arrays (SGPA), to comprehensively map the genetic landscape driving molecular phenotypes of interest. By this approach, a complete yeast genetic mutant array is crossed with fluorescent reporters and imaged on membranes at high density and contrast. Importantly, SGPA enables quantification of phenotypes that are not readily detectable in ordinary genetic analysis of cell fitness. We benchmark SGPA by examining two fundamental biological phenotypes: First we explore glucose repression, in which SGPA identifies a requirement for the Mediator complex and a role for the CDK8/kinase module in regulating transcription. Second, we examine selective protein quality control, in which SGPA identifies most known quality control factors along with U<sub>34</sub> tRNA modification, which acts independently of proteasomal degradation to limit misfolded protein

\*Corresponding authors: Philipp Jaeger, jaeger.phil@gmail.com, Trey Ideker, tideker@ucsd.edu, Randy Hampton, rhampton@ucsd.edu.

#These authors contributed equally.

Lead Contact: Trey Ideker, tideker@ucsd.edu.

**Publisher's Disclaimer:** This is a PDF file of an unedited manuscript that has been accepted for publication. As a service to our customers we are providing this early version of the manuscript. The manuscript will undergo copyediting, typesetting, and review of the resulting proof before it is published in its final citable form. Please note that during the production process errors may be discovered which could affect the content, and all legal disclaimers that apply to the journal pertain.

### AUTHOR CONTRIBUTIONS

P.A.J. conceived and designed the SPOCK collection, developed the SGPA membrane technology, ran the pGAL1 and the CPY SGPA assays and the GLU/GAL fitness screens, performed the data analysis and external data integration; L.O. cloned the CPY reporter strains and performed the follow-up FACS analysis and WB experiments; C.M. and L.R.W. cloned the pGAL1/pTEF1 reporter strains, and created the SPOCK collection; P.A.J., R.Y.H. and T.I. conceived the study; P.A.J., L.O., R.Y.H. and T.I. designed the experiments; P.A.J. created the figures; P.A.J., R.Y.H. and T.I. wrote the manuscript. All authors discussed the results and commented on the manuscript.

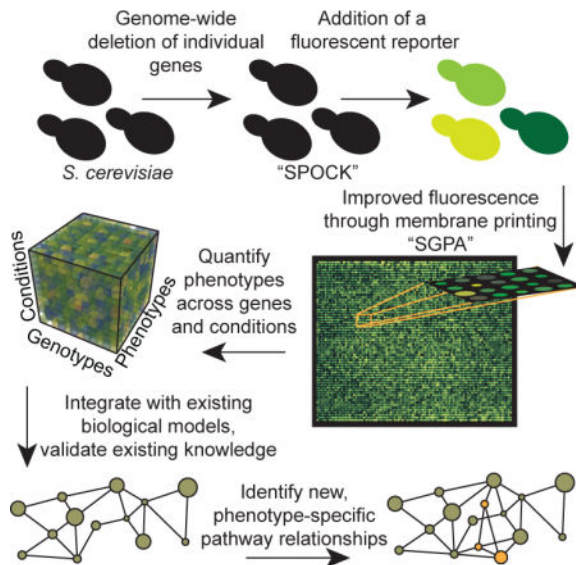
### DECLARATION OF INTERESTS

P.A.J. is the founder of Biocipher<sub>x</sub> Inc., which develops techniques relevant to the research presented. The Regents of the University of California have filed a provisional patent (USPTO 62/507,087) covering parts of the information contained in this article.

production. Integration of SGPA with other fluorescent readouts will enable genetic dissection of a wide range of biological pathways and conditions.

## TOC image

Quantifying an organism's response to gene disruptions enables mapping of molecular pathways. Existing data from yeast is largely constrained to simple "fitness" or "survival" readouts and blind to subtler changes. *Jaeger et al.* present screening technology to obtain data across many phenotypes and conditions rapidly, increasing resolution of pathway maps.



## INTRODUCTION

In yeast (Costanzo et al., 2016; Giaever et al., 2002; Kim et al., 2010; Winzeler et al., 1999) and other microbes (Baba et al., 2006; Schwarzmüller et al., 2014), systematic analysis of large mutant collections has been remarkably successful in mapping the functional genetic architecture of the cell. Such analyses detect alterations in growth caused by genetic mutation, typically by quantifying the sizes of mutant colonies arrayed onto agar (Costanzo et al., 2010; Schuldiner et al., 2005) or by counting barcode tags within a population of cells after competitive liquid growth (Hillenmeyer et al., 2008).

Although colony size and barcode readouts are conducive to screening of cellular fitness, they lack molecular resolution to characterize specific cellular events that fail to induce a growth phenotype. In contrast, optical reporters, including fluorescent probes for pathway activity (Brandman et al., 2012; Jonikas et al., 2009) and tagged proteins (Tkach et al., 2012; Vizeacoumar et al., 2010; Willingham, 2003) can measure a much larger range of phenotypic readouts. Optical readouts are obtained with techniques such as fluorescence activated flow cytometry (Jonikas et al., 2009) or high content microscopy (Aviram et al., 2016; Chong et al., 2015), although they fall short of throughput of high-density cell colony arrays (Bean et al., 2014).

We reasoned that combining the advantages of these approaches might dramatically enhance the power of systematic genetic interrogation and thus developed the Systematic Gene-to-Phenotype Array (SGPA). SGPA brings together comprehensive mutant arrays with optical phenotype reporters by leveraging advantageous signal-to-noise characteristics of microbial colonies grown on synthetic membranes. This technology allows direct assessment of how each gene contributes to a specific phenotype.

As a specific and biologically relevant test of SGPA, we explored two fundamental cellular processes with different phenotypic markers: First, we tested an inducible, tightly controlled pGAL1 promoter, a classic readout of the so called “glucose repression pathway” (Traven et al., 2006). By deploying multiple copies of a pGAL1-fluorescent transcriptional probe per cell, we quantified promoter activation and repression under induced and repressed conditions respectively across approximately 6000 mutant yeast strains. In this context, we found that SGPA enables a broadly useful and sensitive approach to gene discovery, particularly when applied to inherently weak phenotypes such as leaky promoter activity. We identified the highly-conserved Mediator complex as a crucial element in transcriptional control from the pGAL1 promoter. Dynamic module changes in Mediator play a central role in controlling eukaryotic transcription and have been the target of intense research efforts (Allen and Taatjes, 2015). SGPA uncovered a role for the CDK8/kinase module in regulating both promoter repression and induction, depending on environmental context, and identifies module interfaces involved in complex function. This enabled us to build a simple model of CDK8/kinase module control of the GAL1 promoter, advancing our understanding of how this transcriptional element may be regulated over a huge dynamic activity range.

In a second set of experiments, we focused on protein quality control (PQC), a basic process in all domains of life that ensures misfolded proteins are diminished to acceptable levels, either by refolding, degradation, or lowered production (Wolff et al., 2014). One of the most well-studied PQC pathways, the ubiquitin-proteasome system, involves ubiquitin-tagging of proteins and subsequent destruction by the proteasome (Collins and Goldberg, 2017). We probed PQC by deploying a fluorescent, permanently misfolded, but non-toxic protein substrate. Essentially all known PQC components emerged from our SPGA analysis, including the proteasome and the major ubiquitin ligases, and we can show direct contribution of BRE5, a ubiquitin protease co-factor, to control of misfolded protein degradation. Surprisingly, cells deficient in genes underlying the U<sub>34</sub> tRNA modification and urmylation pathway also exhibited a clear PQC phenotype. These gene mutants showed selective accumulation of misfolded proteins, without altering substrate stability or rate of proteasomal degradation, suggesting that selective translational control by modified tRNA serves an underappreciated role in limiting expression of accumulating misfolded proteins.

## DESIGN

Genome-wide technologies to quantify the contribution of gene deletion or gene overexpression to a single (growth) phenotype have been used with great success. High-throughput microscopy- and flow cytometry-based assay systems measure a wide variety of cellular phenotypes. SGPA now combines efficient high-content screening of defined genetic manipulations with the ability to determine a wide range of resulting phenotype changes.

Previous attempts at this approach were limited to promoter-driven fluorescent reporters, required the simultaneous expression of a secondary control reporter to overcome noise, or used slow and expensive fluorescent scanners or low colony density, which severely limited throughput (Göttert et al., 2018; Hendry et al., 2015; Kainth et al. 2009; Sassi et al., 2009). Other genome-wide assays for regulators of protein turnover proved to be extremely data-rich, but required complex tandem degradation assays, followed by scanning or flow cytometry (Khmelinskii et al., 2014; 2012), thus exhibiting an analogous throughput bottleneck. Our experience in differential network biology informed core design principles for SGPA: (1) Leverage existing technology platforms to allow for a swift implementation into existing laboratory settings. (2) Rely on a singular fluorescent reporter channel to avoid unintentional phenotypic signal bias and utilize independent control screens and population-based normalization instead. (3) Maximize throughput by optimizing the physical layout of the underlying mutant collections and very fast image acquisition. By adhering to these principles, we could develop a flexible and fast assay system that can be applied broadly to study phenotypes of interest genome-wide.

## RESULTS

### The Single Plate ORF Compendium Kit enables efficient SGPA

SGPA is built on a super-high-density 6144 yeast colony array format called *Single Plate ORF Compendium Kit* (SPOCK). This format unifies the non-essential gene *Yeast Knock-out* (YKO) (Winzeler et al., 1999) and essential gene *Decreased Abundance by mRNA Perturbation* (DAMP) (Breslow et al., 2008) collections, covering disruptions to >95% of yeast open reading frames, and entails close to 100 wild-type-like controls in the area of a standard 127-by-85 mm microwell plate (Fig. 1A). SPOCK ensures efficient and interspersed placement of essential and non-essential deletion strains (Fig. S1A,B), resulting in homogenous growth phenotypes for both collections (Fig. S1C) and well-mixed distribution of mutant chromosome locations (Fig. S1D).

To enable quantitation of molecular phenotypes, the SPOCK library is transformed with a fluorescent molecular reporter using standard E-MAP mating strategies (Collins et al., 2010). This transformed library is then cultured on a nitrocellulose membrane atop an agar substrate, enabling high-contrast quantitation of the fluorescent signal with free molecule diffusion between agar and colonies (Fig. 1B). This growth setup pairs with an imaging station (Fig. 1C and S2A) to quantify fluorescent reporter signals for all ~6000 mutant strains in <10 seconds per plate (Jaeger et al., 2015). For comparison, high-throughput microscopy of a similar number of mutants in a *GE In Cell Analyzer 2200* requires approximately 1.5 hours. In addition to this ~500-fold increase in speed, the nitrocellulose membrane greatly reduced colony autofluorescence compared to growth on agar (Fig. 1D and S2B), superior even to fluorescence-optimized gels (Jaeger et al., 2015). The improvement in signal is approximately 13-fold (Fig. 1E) without affecting colony size (Fig. S2C), and results were independent from the mode of reporter expression (Fig. S2D). In this way, SGPA combines comprehensive arrays of gene disruptions with fluorescently labeled sensors of phenotype. Parallel execution and analysis of fluorescence-based SGPA and

fitness-based SGA assays does not detect any fitness artifacts (Fig. S3A, B) while substantially increasing signal specificity for molecular events.

### Glucose repression as a model system for eukaryotic transcription control

Although eukaryotic cells can generally metabolize a wide range of carbon sources, many species, including *S. cerevisiae*, prefer fermentation of glucose. When glucose is abundant, they therefore suppress genes involved in respiration, gluconeogenesis, and catabolism of alternative sugars such as galactose (Fig. 2A) through multiple mechanisms known as “glucose repression” (Kayikci and Nielsen, 2015). Incidentally, most of the genes involved in galactose metabolism are essential under galactose-only conditions and readily identified by performing fitness-based mutant analysis (e.g. *gal1*, Fig. 2B). Genes that mediate glucose suppression, on the other hand, show no clear growth phenotype and are thus largely indistinguishable from control strains in classical genetic screens (i.e. *gal80*, Fig. 2B).

To identify genes that maintain glucose repression using SGPA, we utilized a sensitive reporter construct that expresses GFP under control of a pGAL1 promoter sequence (Fig. 2C). The pGAL1 promoter contains four Upstream Activating Sequences (UAS<sub>G</sub>, binding sites for Gal4p), and the TATA box of the *GAL1* gene (Johnston and Davis, 1984). Under galactose-only (inducing) conditions, Gal4p binds to these UAS<sub>G</sub> elements and promotes GAL gene transcription. This leads to GAL gene expression and GFP fluorescence (Fig. 2A, left). In contrast, when glucose is present (repressing conditions), dimerization in the nucleus of the Gal80p repressor inhibits Gal4p binding to the UAS<sub>G</sub>, preventing GAL gene expression and suppressing GFP fluorescence (Fig. 2A, right). Within this framework, fluorescent mutants in the presence of glucose are “Glucose Repression Mutants” (GRMs). Because of tight control of the GAL regulon, we expected weak signal from these mutants and thus delivered the GFP probe as a 2 $\mu$  plasmid. These plasmids themselves have no effect on yeast growth and co-exist with other parasitic plasmids in the yeast nucleus at 20–50 copies (Karim et al., 2013). Importantly, these plasmids replicate and segregate with chromosomes during budding and exhibit nucleosome structure comparable to chromatin (Tong et al., 2006).

### Identifying glucose repression mutants through SGPA

We crossed the pGAL1 reporter plasmid into the SPOCK collection and evaluated colony fluorescence under glucose or galactose, on agar or nitrocellulose. As in our initial technical analysis (Fig. 1D), nitrocellulose improved fluorescence over agar grown colonies (Fig. 2D) and enhanced our ability to detect GRMs under repressed conditions (Fig. 2E). By scattering induced *versus* repressed conditions, we identified three mutant sets (Fig. 2F). The first set we call galactose hypersensitive (GHS) mutants, which have normal fluorescence under glucose and reduced fluorescence under galactose conditions, predominantly due to much reduced colony size. This group is largely overlapping with mutants identified in a traditional fitness-based assay ( $p=3.9\times 10^{-42}$  by hypergeometric test; Fig. 2F, inset), and the intersection is highly enriched for strains deficient in respiration, mitochondrion function (i.e. “mitochondrial inner membrane”  $p=2.33\times 10^{-24}$ ) and galactose metabolism ( $p=9.99\times 10^{-6}$ , see *Processed data and enrichments for the various SGPA*, DataS1).

This is expected, as yeast uses simultaneous respiration and fermentation under galactose conditions (Fendt and Sauer, 2010), an effect similar to enhanced oxidative metabolism observed in galactose-grown human cells (Aguer et al., 2011). A second set of mutants we call galactose tolerant glucose repression mutants (GT-GRM), which have increased pGAL1 promoter activity under glucose but normal fluorescence under galactose. These genes are necessary for glucose repression, but not for galactose metabolism (i.e. *gal80*, Fig. 2F). Third, galactose hypersensitive glucose repression mutants (GHS-GRM) are both necessary for glucose repression and for growth under galactose. We found that most of these mutations affect the Mediator complex, as discussed below (Fig. 2F).

### The CDK8/kinase Mediator module acts as a bimodal transcriptional control unit

Mediator is a modular protein complex that consists of over 20 subunits (Fig. 3A) and exists in all eukaryotes (Allen and Taatjes, 2015). It regulates transcription by RNA polymerase II (RNA Pol II), integrates signals from bound transcription factors, and organizes genomic DNA into topological domains (Allen and Taatjes, 2015). Mediator's composition and structure are flexible, enabling it to perform diverse roles by exchanging subunits and modules dynamically (Allen and Taatjes, 2015). Gal4p-Mediator interactions and genome-wide Mediator occupancy have been used to understand eukaryotic transcriptional regulation (Andrau et al., 2006; Bryant and Ptashne, 2003; Hirst et al., 1999; Holstege et al., 1998; Plaschka et al., 2015; Prather et al., 2005; van de Peppel et al., 2005; Zhu et al., 2006). Based on these studies and comprehensive Chip-seq experiments (Jeronimo et al., 2016; Petrenko et al., 2016), the current model for Mediator function is that a "Tail" module interacts with UAS, a "Head" module interacts with RNA Pol II, and a "Middle" module provides scaffolding and signal transduction. Finally, a "CDK8/Kinase" module negatively regulates the interactions between the Tail and UAS and needs to be released dynamically before Mediator and RNA Pol II can assemble in the preinitiation complex (Jeronimo et al., 2016; Petrenko et al., 2016).

In our SGPA assay, we observed enhanced pGAL1 fluorescence in almost all viable mediator mutant strains (Fig. 3B, C), a phenotype specific to the pGAL1 and entirely undetectable by growth (Fig. 3C). The strongest effect was exerted by CDK8/Kinase module mutants and the peripheral Middle and Tail subunits *nut1* and *med1*. To understand the transcriptional response between the GAL regulatory element and Mediator, we examined expression profiles of 14 Mediator mutant strains across ~3000 transcripts (Kemmeren et al., 2014a). The CDK8/Kinase mutants clearly clustered together with *nut1* and *med1*, suggesting overlapping function (Fig. 3D). To estimate the magnitude of transcriptional change induced by Mediator subunits, we ranked 700 deletion strains based on the variance they induce in expression across half the yeast genome (Fig. 3E). The CDK8/Kinase mutants had the strongest effect of all Mediator subunits, and their effect ranked in the top 2–5% of all yeast gene knockouts. Thus, disruption of the CDK8/Kinase module leads to major transcriptional reorganization but triggers surprisingly modest growth changes under normal glucose conditions (Fig. 3B).

GAL1 expression is tightly repressed under glucose and exhibits invariance to a wide range of mutations affecting transcription (Fig. S4A). For example, GAL1 mRNA appeared



unchanged in some Mediator mutants (not including the CDK8/kinase module) in two studies (Kemmeren et al., 2014b; Lenstra et al., 2011) using traditional microarray mRNA quantification (Fig. S4B), highlighting the potential of SGPA in amplifying very weak promoter signal. Chip-seq data from CDK8/Kinase module mutants (Jeronimo et al., 2016) lends support to the leaky pGAL1 phenotype model (Fig. 3F) suggested by SGPA: Under glucose repressed conditions, Mediator binding in the GAL1 promoter region is virtually absent (Fig. S4C, Mediator/wt), while deletion of a CDK8/Kinase gene (*ssn2*), increases GAL11 presence at the UAS<sub>G</sub> (Fig. S4C, Gal11/*ssn2*), an effect not observed, for example, at the neighboring gene FUR4.

### Using SGPA to examine protein quality control

As a second case study, we sought to genetically dissect molecular phenotypes related to Carboxypeptidase Y (CPY), a well-established substrate for the study of protein quality control pathways (Heck et al., 2010; Plemper et al., 1997; Stolz and Wolf, 2012). A permanently misfolded state in the normal CPY protein is induced by a single amino-acid substitution denoted CPY\*. Subsequent removal of the endoplasmic reticulum import-signal sequence (ss) and addition of Green Fluorescent Protein (GFP) results in the model cytoplasmic misfolded protein ssCPY\*-GFP (Fig. 4A). Normally, this misfolded protein is rapidly degraded by PQC machinery, whereas disturbances in PQC are identified by accumulation of ssCPY\*-GFP (Stolz and Wolf, 2012). Specifically, ssCPY\*-GFP is marked for degradation by the San1p and Ubr1p ubiquitin ligases in the nucleus *versus* cytosol, respectively (Heck et al., 2010), while deubiquitinating enzymes like Ubp3p promote its stabilization (Fig. 4B).

We used SGPA to comprehensively evaluate the effect of yeast gene mutations on levels of ssCPY\*-GFP integrated as a single copy at the ADE2 locus. To eliminate genes that have general effects on GFP expression or brightness rather than roles in PQC, we assessed the differential fluorescence between each mutant expressing either misfolded ssCPY\*-GFP or GFP alone (Fig. 4C). In a total of 274 gene deletion mutants, we observed significant changes in GFP colony fluorescence relative to control (Fig. 4C and S5A, DataS1).

### Validation against known PQC factors and robustness to substrate location

As a first validation of these results, we scored the extent to which the SGPA gene set recovered known components of protein quality control, including the established ubiquitinating/deubiquitinating enzymes and the proteasome complex (DataS1). The approach recovered mutant strains for both the ubiquitin ligases (*san1* and *ubr1*) and the deubiquitinating enzyme (*ubp3*) which played opposing roles on the test substrate: loss of the known ligases resulted in elevated GFP levels, while loss of the deubiquitinating enzyme resulted in decreased GFP levels (Fig. 4D, E), and altered degradation kinetics (Fig. 4F, *pdr5* serves as 'wildtype' control). SGPA also recovered 70% (21/30) of essential proteasome complex members based on a strong increase in GFP fluorescence in the hypomorphic mutant strains (Figs. 4G–J). In contrast, we noted very little change in cellular fitness due to deletion of any of these genes, demonstrating the difficulty in studying a basic biological process such as PQC with a simple assay based only on cellular growth.



We next sought to assess the robustness of these results to defined changes in subcellular location of the misfolded protein. Accordingly, we performed two independent follow-up screens with well characterized substrate derivatives: First, we used a modified fluorescent substrate predominantly localized in the cytosol ( ssCPY\*-GFP-NES, ssCPY\*-GFP with a Nuclear Export Signal (Heck et al., 2010)). Second, we deleted the nuclear ubiquitin ligase SAN1 across all mutants (Heck et al., 2010; Prasad et al., 2010), which is involved in proteasome-dependent degradation of aberrant nuclear proteins ( ssCPY\*-GFP *san1* , Fig. 5A). All three screens yielded highly overlapping hits ( $p \ll 10^{-8}$ ), indicating that misfolded CPY identification and degradation employ similar mechanisms independent of subcellular localization (Fig. 5B, S5A, B). Due to this overall similarity, we took the union of all three screens to create a unified data set of 556 mutants with either significantly increased or decreased fluorescence compared to wildtype (Fig S5A, DataS1).

### Functional analysis of PQC mutants implicates BRE5 and tRNA modification genes

A total of 312 *versus* 244 mutants were associated with decreased or increased ssCPY\* fluorescence (Fig. 5B, S5A). Functional analysis of the 312 mutants associated with decreased ssCPY\* levels did not identify any enriched biological processes among the corresponding disrupted genes using Gene Ontology SLIM (Ashburner et al., 2000; The Gene Ontology Consortium, 2015) (data not shown). Regardless, further investigation of these genes revealed those with functional relevance to protein quality control (Fig. S6A). For instance, lowered ssCPY\*-GFP levels were observed in the *bre5* mutant, which had not been previously linked to PQC pathways, although Bre5p forms a complex with the Ubp3p ubiquitin-specific protease (Fig. 4C–F, S6A–C). This effect was robust and strong enough to be visible to the naked eye (Fig. 4E) and supported by protein degradation pulse-chase experiments, both in Western Blot (Fig. 4F) and FACS experiments (Fig. S6C).

Analysis of the 244 mutants associated with increased ssCPY\*-GFP levels was particularly informative, indicating many genes potentially functioning in protein degradation or quality control. The genes were enriched for biological processes (based on GO SLIM enrichment), broadly organized into four superclasses: (1) Ubiquitination/Proteasome; (2) RNA processing; (3) Unfolded protein binding; and (4) Chromatin/Transcription (Fig. 5B and S7A). Mutant fluorescence signatures were robust across superclasses and screens (Fig. 5C), further supporting largely location-independent function of the PQC machinery and reliability of the assay. The only significantly different results were obtained for the set of “Chromatin/Transcription” mutants in the ssCPY\*-GFP-NES screen (Fig. 5C, ANOVA followed by Dunnett’s multiple comparisons test), supportive of the idea that excluding misfolded protein from the nucleus could reduce its direct effect on DNA modifications and transcription. We also performed an enrichment test against known protein complexes. Besides proteasome-related complexes we observed significant enrichment for the Elongator Holoenzyme Complex, the DUBm Complex and the ESCRT Complex (Fig. 6A and S7B, GO slim terms, Fisher’s exact test).

In both types of functional analyses, we observed a overrepresentation of genes involved in U<sub>34</sub> tRNA modification (Fig. 6A and S7A, B), which included members of the urmylation and elongator complex genes (Kirchner and Ignatova, 2014). The urmylation gene (URM1)

is highly conserved from yeast to humans with a unique dual-function role, acting both as a protein modifier in ubiquitin-like urmylation and as a sulfur donor for tRNA thiolation (Juedes et al., 2016). Together with the Elongator pathway, the urmylation pathway forms 5-methoxy-carbonyl-methyl-2-thio (mcm5s2) modified wobble uridines (U<sub>34</sub>) in tRNA anticodons (Jüdes et al., 2015), important for structural integrity of the cell, decoding efficiency, and mRNA translation accuracy (Klassen et al., 2016). Urmylation and elongator complex mutants showed SGPA phenotypes nearly as strong, and in some cases stronger, than the ubiquitination-deficient *ubr1* and *san1* mutants (Fig. 6B), a behavior largely reproducible in all three ssCPY\* screens (Fig. 6C). Two of the tRNA modification mutants (*elp4* and *ncs2*) were independently validated through the existence of ‘dubious ORF’ mutants in the SPOCK collection that overlap partially with the respective gene locus (*yp1102c* and *yn1120c*), causing the same loss of gene product and identical phenotype. We found that temporal expression patterns (Brar et al., 2012) of tRNA modification genes were very different from those of the proteasome (Fig. 7A), and that deletion of tRNA modification or proteasomal genes induced very different expression responses (Kemmeren et al., 2014a) (Fig. 7B). Despite their similar effects on ssCPY\*-GFP fluorescence, these findings suggest that tRNA modification and proteasomal degradation have distinct and non-simultaneous effects on protein quality control.

### Protein accumulation in U<sub>34</sub> tRNA deficient cells is not due to altered degradation rate

Recent findings suggest that U<sub>34</sub> tRNA deficiency slows translation and can induce misfolding in wildtype proteins, leading to buildup of aggregates and proteotoxic stress (Klassen et al., 2016; Nedialkova and Leidel, 2015). However, in our study the protein substrate was constitutively and permanently misfolded (Stolz and Wolf, 2012), suggesting that mechanisms other than alteration of native folding configurations were responsible for the observed accumulation of ssCPY\*-GFP.

To evaluate the importance of U<sub>34</sub> tRNA deficiency on ssCPY\*-GFP degradation, we performed cycloheximide chase experiments on ssCPY\*-GFP in the candidate mutants, to directly evaluate effects on protein stability (Fig. 7C). Remarkably, neither the elongator complex nor urmylation deficient mutants showed any effects on ssCPY\*-GFP stability. These behaviors were in striking contrast to the ubiquitin-proteasome mutants detected in the screen, which showed clear changes in substrate degradation (Fig. 7C).

If misfolded protein degradation is not impaired, we reasoned that the observed increase in ssCPY\*-GFP in the mutants might be due to increased protein production. To test this hypothesis, we measured the steady-state concentration of ssCPY\*-GFP *via* FACS in a set of freshly transformed U<sub>34</sub> tRNA modification deficient mutants. To exclude screen-specific artifacts, mutants were generated through direct transformation of the ssCPY\*-GFP expression plasmid (or the analogous plasmid expressing GFP as control) into the respective mutant strains instead of going through the mass-mating and selection process. We observed significantly higher steady-state concentrations of ssCPY\*-GFP in a wide range of elongator and urmylation deficient mutants (Fig. 7D, S7C), strongly supporting our initial findings with SGPA (Fig. 6B). This finding was again confirmed when using a different model protein: a truncated form of the glycolytic enzyme Gnd1(tGnd1) which is a short-

lived substrate for the E3 ubiquitin ligases San1p and Ubr1p (Heck et al., 2010) (Fig. 7E). Importantly, the elevation of steady state was specific for the misfolded substrates; no elevation of identically expressed GFP was observed over the wild-type control.

A >3-fold increase in ssCPY\*-GFP concentration (i.e. as observed with the elongator mutant *elp2*) on the background of normal proteasomal degradation could indicate hyperactive rather than slowed translation, exerting significant pressure on the translational machinery. To test if translation is indeed changed in U<sub>34</sub> tRNA modification deficient cells, we exposed these cells to two different compounds that induce translational stress at sub-toxic concentrations: hygromycin B, which stabilizes the tRNA-ribosomal acceptor site, thereby inhibiting proper ribosome translocation; and canavanine, a non-proteinogenic amino acid that can replace L-arginine during translation, thereby producing structurally aberrant proteins. Remarkably, the same urmylation and elongator complex mutants that exhibit the strongest increase in ssCPY\*-GFP accumulation are hypersensitive to these compounds (Fig. 7F), suggesting that this class of mutants are abnormally affected by increased load of misfolded proteins.

## DISCUSSION

Our first application of SGPA to regulation of *GALI* promoter activity recovered most of the known biology of galactose metabolism and regulatory elements covering Gal4p-*GALI* promoter control. The weak signal expected from a repressed promoter represents an ideal test case for the sensitivity of the new membrane technology and yielded superior results to agar-based imaging. Functionally, our results support the findings of recent studies suggesting an independent role for the CDK8/kinase Mediator module in repressing Tail interaction with UAS (Jeronimo et al., 2016; Petrenko et al., 2016). Our data also highlight a unique, bi-modal role of the CDK8/Kinase module in the GAL regulon: Since the CDK8/Kinase module is necessary for the activation of Gal4p transcription factor activity as well as suppression of the Tail-UAS<sub>G</sub>- and Head-RNA Pol II-interactions, this Mediator module is ideally suited to exert the extraordinarily tight control of the “galactose switch”. Interference with CDK8/Kinase module function through deletion of any of its members renders the galactose switch both leaky and un-flippable. The glucose repression defect phenotype was extremely weak. This emphasizes that, depending on the magnitude of the expected phenotypic change, it is wise to adapt the reporter construction accordingly: In our *GALI* regulon case, a high copy, signal amplifying 2 $\mu$  plasmid proved beneficial, but in other situations such as when probing tagged proteins (see the CPY section) or when the reporter is toxic on its own, low copy CEN plasmids or chromosomal integration with modestly strong promoters may be better suited to not overload the cell with reporter “stress”.

It will be informative to evaluate the role of Nut1p and Med1p in mediating CDK8/Kinase module function during glucose repression. While our data show the most comprehensive effects for the CDK8/Kinase mutants, most of the Tail module mutants are DAMP mutants and thus not totally depleted for the respective proteins. It is thus conceivable that complete loss of other Tail subunits could phenocopy CDK8/Kinase mutants, however those strains are non-viable and would need to be constructed in a dynamically inducible fashion. Overall, these data demonstrate the usefulness of SGPA to identify functional complexes

that mediate specific roles in transcription control and to generate many leads on the organization of eukaryotic transcription control. Given the recent appreciation of Mediator and Mediator mutations in several developmental diseases (Wang et al., 2013), it will be interesting to see how far the GAL regulon control model extends into a more general model of gene repression and activation. Intriguingly, MED12, the human homolog of yeast *SRB8*, has recently been identified as a cancer hotspot (Lim et al., 2014; Ng et al., 2015; Siraj et al., 2017) and has been implicated in affecting the response to multiple cancer drugs (Huang et al., 2012). Given that CDK8/Kinase mutations have a strongly deregulatory effect on global and de-repressing effect on GAL regulon transcription in yeast, it is possible that similar de-repression of tightly controlled oncogenes could occur in humans. Future molecular work will be needed to better understand the functional implications of this effect.

By applying SPGA analysis to misfolded protein phenotypes, we demonstrated two new aspects of this highly conserved process. First, the existence of negative factors Ubp3 and Bre5 that normally diminish degradation, allowing for a more nuanced approach to triage. Second, and more surprising, a specific involvement of genes associated with U<sub>34</sub> tRNA modification in the accumulation of misfolded proteins, indicating that tRNAs and other ubiquitin-like modifiers could make interesting targets for future therapeutic interventions to combat the numerous proteostasis related diseases. Previously, deficiency in U<sub>34</sub> tRNA modifications had been implicated in slowing translation of certain wildtype proteins, leading to misfolding and proteotoxic stress (Klassen et al., 2016; Nedialkova and Leidel, 2015). This led to the assumption that U<sub>34</sub> tRNA modification deficiency exerts predominantly proteotoxic stress *via* the accumulation of protein aggregates. Here we show instead that U<sub>34</sub> tRNA modification mutants have close to normal degradative capacity and proteasome speed when challenged with a single, non-toxic misfolded protein substrate. Rather than slowing translation, accumulation of ssCPY\*-GFP appears to be driven by increased production in the deficient cells. Consistent with this model, the U<sub>34</sub> tRNA modification deficient cells were sensitive to other translation stressors such as sub-toxic canavanine or hygromycin treatment. This study opens the possibility that U<sub>34</sub> tRNA modifications plays a previously unappreciated role in controlling production of correctly folded proteins, and thus can act both as accelerators and breaks on protein production, potentially enabling fine-tuning of expression in response to protein levels (Fig. 5G). Future, more detailed polysome analysis or ribosomal profiling studies are needed to clarify the exact mechanism and functional relevance underlying this phenomenon.

High-throughput screens of yeast fitness have revolutionized our ability to map the genomic landscape and to identify gene and pathway relationships relevant to cell growth. Recent efforts emphasize the importance of targeted conditional screens to increase hit rate and to build a deeper understanding of genetic dependencies when the cell faces relevant external stressors (Bandyopadhyay et al., 2010; Bean and Ideker, 2012; Ideker and Krogan, 2012; Kramer et al., 2017; Srivas et al., 2013). Examples of screens exploring some of these different angles include gene-gene (Costanzo et al., 2016), gene-drug (Hillenmeyer et al., 2008; Lee et al., 2014), gene-metabolome (Mülleder et al., 2016), or triple-genetic interactions (Braberg et al., 2014). However, fitness-based screening efforts are inherently limited to a single readout – colony growth – restraining the possible richness of the data obtainable, while highly specialized screens (e.g. high content microscopy, expression

profiling, or mass spectroscopy) are extremely slow and cumbersome when applied across thousands of mutant strains. SGPA overcomes these limitations.

Beyond the study of promoter control and protein degradation and folding, other phenotypic markers are readily conceivable: Organelle function (e.g. lysosome, autophagosome, peroxysomes) could be assessed by targeting GFP-tagged proteins to specific compartments and monitoring GFP degradation (or by using any other pH sensitive marker); expression could be followed by measuring GFP-tagged levels of the protein; protein-protein interactions could be assessed *in vivo* by using Bimolecular Fluorescence Complementation or fluorescent variants of Yeast-Two-Hybrid technology; and so on. This versatility has far reaching implications for the utility of yeast screening in drug discovery, as large-scale discovery data sets can be generated at low cost and in short time and targeted specifically to phenotypes of interest. Finally, the SGPA platform is in principle transferable to other species (e.g. *S. pombe*), including to other domains (*C. reinhardtii*) or kingdoms (*E. coli*) of life, since systematic mutant collections are becoming more widespread in those organisms.

### Limitations

While the final imaging step is extremely fast and the overall process can be efficiently parallelized, an individual SGPA screen from start to finish can take up to two weeks (including growing up the SPOCK collection, crossing in the fluorescent marker(s), followed by the appropriate selection steps). When accounting for growth saturation at each step, this translates into ~100 yeast generations. If a phenotype of interest elicits a strong counter-selective pressure, then this number of generations may be sufficient to give rise to a masking mutation. We describe an effect like that in detail in a companion manuscript (Neal et al., in press).

This is of course not unique to SGPA, but inherently affects all high-throughput approaches that require a significant number of generations to pass between an event (i.e. a gene suppression experiment) and its readout (i.e. after expansion of the cell line). To some degree this evolutionary adaptation to the phenotype ‘fitness’ has already occurred in the yeast deletion collections that are part of SPOCK (Teng et al., 2011) and as such should be considered a hidden variable in all derived high-throughput yeast deletions screens. This problem of adaptation could be overcome by designing inducible phenotype reporters for SGPA, controlled for example by galactose or tetracycline, however these “conditions” then in turn require careful additional experiments to control for non-specific inducer effects. We thus always strongly recommend the inclusion of positive controls.

## STAR METHODS

### CONTACT FOR REAGENTS AND RESOURCE SHARING

Further information and requests for resources and reagents should be directed and will be fulfilled by the Lead Contact, Trey Ideker (tideker@ucsd.edu).

## EXPERIMENTAL MODEL AND SUBJECT DETAILS

**SPOCK collection and high-throughput yeast screens**—Strains from the YKO and DAmP collections (GE Dharmacon, Lafayette, CO) were grown on YPAD medium with 100 µg/ml G418 at 96 colony density and then manually re-arrayed to remove blank spaces, non-growing strains, and duplicates, resulting in the SPOCK collection. A complete strain list and location map can be found in the Supplemental Data File. The 96 well plates were then re-pinned and condensed to 6144 colony density using the Rotor HAD (Singer Instruments, Taunton, UK). Mating with the CPY or pGAL1 query strains and selection were performed using standard E-MAP procedures (Collins et al., 2010), except that all incubation steps took place over-night at room temperature to avoid overgrowth. After double mutant selection, strains were pinned onto agar (for fitness measurements) or onto 0.45µm nitrocellulose membrane (BioRad, Hercules, CA; for fluorescence measurements). The membrane was pre-wetted with selection media and rolled onto the agar surface to avoid bubble formation.

**Strains and Plasmids**—The *Saccharomyces cerevisiae* strains used in this study are listed in Supplemental Table S1. Media preparation, genetic and molecular biology techniques were carried out using standard methods: Yeast strains were cultured using yeast extract/peptone/dextrose (YPD) at 30°C. Majority of the deletion strains used were in the BY4741 (MATa *ura3 0 leu2 0 his3 1 met15 0*) background derived from the Resgen Deletion Collection (GE Dharmacon) except the Y7092 query strain. The Y7092 strains carried the respective insertions for each of the generated screens using standard LiOAc protocols for transformation:

*ade2* ::URA3-ADE2

*ade2* ::URA3-ADE2-pTDH3- ssCPY\*

*ade2* ::URA3-ADE2-pTDH3- ssCPY-GFP

*ade2* ::URA3-ADE2-pTDH3- ssCPY-NES-GFP

*ade2* ::URA3-ADE2-pTDH3- ssCPY-GFP *san1* ::cNAT

The plasmid cytoplasmic Carboxypeptidase-Y protein ssCPY\*-GFP (pRH2081) was provided by D. Wolf (University of Stuttgart, Stuttgart, Germany). tGND1 (pRH2476), and ssCPY\*-GFP-NES (pRH2557) was provided by D. Hampton (University of California San Diego, La Jolla, CA). Plasmids were heat-shock transformed into competent *E. coli* (DH5α), recovered using standard Mini-Prep protocols (Promega), and re-transformed into yeast cells using standard procedures. Competent colonies were selected with the appropriate selection conditions.

## METHOD DETAILS

**Gel preparation, selection markers, and media**—Bacto™ agar (#214040, BD Biosciences, San Jose/CA) was used as the gelling agent. Supplemental reagents and media were Bacto™ yeast extract (#212720, BD Biosciences), Bacto™ peptone (#211820, BD Biosciences), Difco™ Dextrose/Glucose (#215520, BD Biosciences), Difco™ Yeast nitrogen base without amino acids (#291920, BD Biosciences) and Difco™ Yeast nitrogen base without amino acids and ammonium sulfate (#233520, BD Biosciences). In case of the



galactose experiments, glucose (2%) was replaced with an equal percentage galactose (2%). Synthetic complete (SC) or SC-dropout media were prepared following standard procedures using amino acids from Sigma-Aldrich. If indicated, selective pressure was maintained using geneticin (G418, KSE Scientific, Durham/NC), S-(2-Aminoethyl)-L-cysteine hydrochloride (S-AEC, A2636, Sigma-Aldrich), or L-(+)-(S)-Canavanine (Can, C9758, Sigma-Aldrich) at the indicated concentrations. Gelling, supplemental, and media reagents were mixed in ddH<sub>2</sub>O and autoclaved for 15min at 121°C before use; selective drugs were added after the liquid gel solution cooled to below 60°C in a water bath.

**White-light imaging station**—Images of gels and yeast colonies were acquired using a digital imaging setup described previously (Bean et al., 2014) with a commercially available SLR camera (18 Mpixel Rebel T3i, Canon USA Inc., Melville/NY) with an 18–55 mm zoom lens. We used a white diffusor box with bilateral illumination and an overhead mount for the camera in a dark room. Images were taken in highest quality, 8-bit color-depth JPEG.

**Fluorescent imaging station**—Images of gels were acquired using a custom fluorescent digital imaging setup described previously (Jaeger et al., 2015). We used a commercially available SLR camera (20.2 Mpixel EOS 6D, Canon) with a 100mm f/2.8 macro lens (Canon) and a green band-pass filter (BP532, Midwest Optical Systems, Inc., Palatine/IL). We used a 460nm LED panels (GreenEnergyStar, Vancouver BC, Canada) with a ¼ white diffusion filter (#251, Lee Filters, Burbank/CA, USA) for 45° bilateral illumination (205560, Kaiser Fototechnik GmbH & Co. KG, Buchen, Germany), and an overhead mount for the camera (205510, Kaiser) in a dark room. Images were taken in highest quality, 8-bit color-depth JPEG.

**Image analysis**—Colony information was collected after images were normalized, spatially corrected, and quantified using a set of previously published custom algorithms, aka “The Colony Analyzer Toolkit” (Bean et al., 2014). Digital images were cropped and assembled in Photoshop and Illustrator (CS6, Adobe Inc., San Jose/CA) for publication.

**Western Blot Analysis**—Cycloheximide chase degradation assays were performed in a manner previously described (Heck et al., 2010). Yeast cells were grown to log-phase cultures and cycloheximide was added to a final concentration of 50 µg/mL. At the indicated time points, cells were collected by centrifugation and lysed with 100 µl of SUME [1% SDS, 8 M UREA, 10mM MOPS, PH 6.8, 10mM EDTA] with protease inhibitors (142 µM TPCK, 100 µM leupeptin, 76 µM pepstatin) and 0.5-mm glass beads, followed by vortexing for 5 min at 4°C and addition of 100 µl of 2× USB [75 mM Mops, pH 6.8, 4% SDS, 200 mM DTT, 0.2 mg/mL bromophenol blue, 8 M urea].

The bead slurry was heated to 80°C for 5 min and then clarified by centrifugation before separation by SDS/PAGE and subsequent immunoblotting with monoclonal anti-GFP (Clontech).

**Flow Cytometry Steady State**—Cell cultures were grown to low log phase (OD<sub>600</sub> = 0.1) in extract/peptone/destrose (YPD) at 30°C. GFP fluorescence levels were measured in

living cells (10,000 per sample) with a BD Biosciences flow cytometer and analyzed with Flowjo software.

**Phenotyping**—To evaluate cell growth, indicated strains were grown at 30°C in YPD medium overnight. Cultures were then diluted, grown to log-phase, and a total of 0.3 OD units was pelleted and resuspended in 250 µl of sterile water. Five-fold dilutions were then performed in a 96-well plate and spotted onto on the indicated media. Studies of canavanine sensitivity were conducted using minimal media (agarose/yeast nitrogenous bases) with the minimal amino acids (His/Leu/Met/Ura), and 0.2 µg/ml of canavanine (Sigma) grown at 30°C for 3 days. Indicated strains for hygromycin B studies were grown in YPD and 62.5 µg/ml of hygromycin B (Invitrogen) at 30°C for 3 days.

**Ribosome occupancy and mRNA expression data analysis**—Ribosome occupancy data was available publicly (Brar et al., 2012). We computed average ribosome occupancy data for selected ORF's annotated with the specific functions in GO/Yeastmine (see Supplemental Data File). Expression data for a large set of deletion mutants was available publicly. We extracted the expression profile correlations for mutants that were part of Mediator or our 244 proteasome hits and performed unsupervised clustering.

## QUANTIFICATION AND STATISTICAL ANALYSIS

Quantification and statistical analysis were performed in MatLab (Mathworks, Natick/MA). Details of the statistical analysis can be found in the figures, figure legends and the results section of the text. Statistical test and number of samples are indicated whenever appropriate.

## DATA AND SOFTWARE AVAILABILITY

All data for the galactose and CPY screens is available in Supplemental Data File 1. Representative images for all screens are available online at Mendeley Data (<http://dx.doi.org/10.17632/w2rm2fmzz7.1>).

## Supplementary Material

Refer to Web version on PubMed Central for supplementary material.

## Acknowledgments

We thank Joris Van de Haar for his contribution to establishing the SGPA system and Jason F. Kreisberg for his critical comments on the manuscript. We thank Kate Licon for her tireless efforts to keep the lab running at peak performance always and Leonard S. Nimoy for his lifelong ambassadorship for science (the SPOCK collection shall be named in his honor). Funding for this study was provided by R01ESO14811 (T.I.), R01GM084279 (T.I.), R01GM092748 (R.Y.H.), 5R37DK051996 (R.Y.H.), R41TR001908 (P.A.J), and T32GM007240 (L.O).

## References

- Aguer C, Gambarotta D, Mailloux RJ, Moffat C, Dent R, McPherson R, Harper ME. Galactose Enhances Oxidative Metabolism and Reveals Mitochondrial Dysfunction in Human Primary Muscle Cells. *PLoS One*. 2011; 6:e28536–11. [PubMed: 22194845]
- Allen BL, Taatjes DJ. The Mediator complex: a central integrator of transcription. *Nat Rev Mol Cell Biol*. 2015; 16:155–166. [PubMed: 25693131]

- Andrau JC, van de Pasch L, Lijnzaad P, Bijma T, Koerkamp MG, van de Peppel J, Werner M, Holstege FCP. Genome-Wide Location of the Coactivator Mediator: Binding without Activation and Transient Cdk8 Interaction on DNA. *Mol Cell*. 2006; 22:179–192. [PubMed: 16630888]
- Ashburner M, Ball CA, Blake JA, Botstein D, Butler H, Cherry JM, Davis AP, Dolinski K, Dwight SS, Eppig JT, et al. Gene Ontology: tool for the unification of biology. *Nat Genet*. 2000; 25:25–29. [PubMed: 10802651]
- Aviram N, Ast T, Costa EA, Arakel EC, Chuartzman SG, Jan CH, Haßdenteufel S, Dudek J, Jung M, Schorr S, et al. The SND proteins constitute an alternative targeting route to the endoplasmic reticulum. *Nature*. 2016; 540:134–138. [PubMed: 27905431]
- Baba T, Ara T, Hasegawa M, Takai Y, Okumura Y, Baba M, Datsenko KA, Tomita M, Wanner BL, Mori H. Construction of *Escherichia coli* K-12 in-frame, single-gene knockout mutants: the Keio collection. *Mol Syst Biol*. 2006; 2:473–11.
- Bandyopadhyay S, Mehta M, Kuo D, Sung MK, Chuang R, Jaehnig EJ, Bodenmiller B, Licon K, Copeland W, Shales M, et al. Rewiring of genetic networks in response to DNA damage. *Science*. 2010; 330:1385–1389. [PubMed: 21127252]
- Bean GJ, Ideker T. Differential analysis of high-throughput quantitative genetic interaction data. *Genome Biol*. 2012; 13:R123. [PubMed: 23268787]
- Bean GJ, Jaeger PA, Bahr S, Ideker T. Development of Ultra-High-Density Screening Tools for Microbial “Omics”. *PLoS One*. 2014; 9:e85177. [PubMed: 24465499]
- Braberg H, Alexander R, Shales M, Xu J, Franks-Skiba KE, Wu Q, Haber JE, Krogan NJ. Quantitative analysis of triple-mutant genetic interactions. *Nature Protocols*. 2014; 9:1867–1881. [PubMed: 25010907]
- Brandman O, Stewart-Ornstein J, Wong D, Larson A, Williams CC, Li GW, Zhou S, King D, Shen PS, Weibezahn J, et al. A Ribosome-Bound Quality Control Complex Triggers Degradation of Nascent Peptides and Signals Translation Stress. *Cell*. 2012; 151:1042–1054. [PubMed: 23178123]
- Brar GA, Yassour M, Friedman N, Regev A, Ingolia NT, Weissman JS. High-resolution view of the yeast meiotic program revealed by ribosome profiling. *Science*. 2012; 335:552–557. [PubMed: 22194413]
- Breslow DK, Cameron DM, Collins SR, Schuldiner M, Stewart-Ornstein J, Newman HW, Braun S, Madhani HD, Krogan NJ, Weissman JS. A comprehensive strategy enabling high-resolution functional analysis of the yeast genome. *Nat Meth*. 2008; 5:711–718.
- Bryant GO, Ptashne M. Independent recruitment *in vivo* by Gal4 of two complexes required for transcription. *Mol Cell*. 2003; 11:1301–1309. [PubMed: 12769853]
- Chong YT, Koh JLY, Friesen H, Duffy K, Cox MJ, Moses A, Moffat J, Boone C, Andrews BJ. Yeast Proteome Dynamics from Single Cell Imaging and Automated Analysis. *Cell*. 2015; 161:1413–1424. [PubMed: 26046442]
- Collins GA, Goldberg AL. The Logic of the 26S Proteasome. *Cell*. 2017; 169:792–806. [PubMed: 28525752]
- Collins, SR., Roguev, A., Krogan, NJ. Quantitative Genetic Interaction Mapping Using the E-MAP Approach. Elsevier Inc; 2010.
- Costanzo M, Baryshnikova A, Bellay J, Kim Y, Spear ED, Sevier CS, Ding H, Koh JLY, Toufighi K, Mostafavi S, et al. The genetic landscape of a cell. *Science*. 2010; 327:425–431. [PubMed: 20093466]
- Costanzo M, Van der Sluis B, Koch EN, Baryshnikova A, Pons C, Tan G, Wang W, Usaj M, Hanchard J, Lee SD, et al. A global genetic interaction network maps a wiring diagram of cellular function. *Science*. 2016; 353:aaf1420. [PubMed: 27708008]
- Fendt SM, Sauer U. Transcriptional regulation of respiration in yeast metabolizing differently repressive carbon substrates. *BMC Systems Biology*. 2010; 4:12. [PubMed: 20167065]
- Giaever G, Chu AM, Ni L, Connelly C, Riles L, Véronneau S, Dow S, Lucau-Danila A, Anderson K, André B, et al. Functional profiling of the *Saccharomyces cerevisiae* genome. *Nature*. 2002; 418:387–391. [PubMed: 12140549]
- Göttert H, Mattiazzi Usaj M, Rosebrock AP, Andrews BJ. Reporter-Based Synthetic Genetic Array Analysis: A Functional Genomics Approach for Investigating Transcript or Protein Abundance

- Using Fluorescent Proteins in *Saccharomyces cerevisiae*. *Methods Mol Biol.* 2018; 1672:613–629. [PubMed: 29043651]
- Heck JW, Cheung SK, Hampton RY. Cytoplasmic protein quality control degradation mediated by parallel actions of the E3 ubiquitin ligases Ubr1 and San1. *Proc Natl Acad Sci USA.* 2010; 107:1106–1111. [PubMed: 20080635]
- Hendry JA, Tan G, Ou J, Boone C, Brown GW. Leveraging DNA damage response signaling to identify yeast genes controlling genome stability. *G3 (Bethesda).* 2015; 5:997–1006. [PubMed: 25721128]
- Hillenmeyer ME, Fung E, Wildenhain J, Pierce SE, Hoon S, Lee W, Proctor M, St Onge RP, Tyers M, Koller D, et al. The chemical genomic portrait of yeast: uncovering a phenotype for all genes. *Science.* 2008; 320:362–365. [PubMed: 18420932]
- Hirst M, Kobor MS, Kuriakose N, Greenblatt J, Sadowski I. GAL4 is regulated by the RNA polymerase II holoenzyme-associated cyclin-dependent protein kinase SRB10/CDK8. *Mol Cell.* 1999; 3:673–678. [PubMed: 10360183]
- Holstege FC, Jennings EG, Wyrick JJ, Lee TI, Hengartner CJ, Green MR, Golub TR, Lander ES, Young RA. Dissecting the regulatory circuitry of a eukaryotic genome. *Cell.* 1998; 95:717–728. [PubMed: 9845373]
- Huang S, Hölzel M, Knijnenburg T, Schlicker A, Roepman P, McDermott U, Garnett M, Grenrum W, Sun C, Prahallad A, et al. MED12 Controls the Response to Multiple Cancer Drugs through Regulation of TGF- $\beta$  Receptor Signaling. *Cell.* 2012; 151:937–950. [PubMed: 23178117]
- Ideker T, Krogan NJ. Differential network biology. *Mol Syst Biol.* 2012; 8:565. [PubMed: 22252388]
- Jaeger PA, McElfresh C, Wong LR, Ideker T. Beyond agar: gel substrates for microbial growth experiments with improved optical clarity and drug efficiency and reduced autofluorescence. *Appl Environ Microbiol.* 2015; 81:5639–5649. [PubMed: 26070672]
- Jeronimo C, Langelier MF, Bataille AR, Pascal JM, Pugh BF, Robert F. Tail and Kinase Modules Differently Regulate Core Mediator Recruitment and Function *In Vivo*. *Mol Cell.* 2016; 64:455–466. [PubMed: 27773677]
- Johnston M, Davis RW. Sequences that regulate the divergent GAL1-GAL10 promoter in *Saccharomyces cerevisiae*. *Mol Cell Biol.* 1984; 4:1440–1448. [PubMed: 6092912]
- Jonikas MC, Collins SR, Denic V, Oh E, Quan EM, Schmid V, Weibezahn J, Schwappach B, Walter P, Weissman JS, et al. Comprehensive Characterization of Genes Required for Protein Folding in the Endoplasmic Reticulum. *Science.* 2009; 323:1693–1697. [PubMed: 19325107]
- Juedes A, Bruch A, Klassen R, Helm M, Schaffrath R. Sulfur transfer and activation by ubiquitin-like modifier system Uba4-Urm1 link protein urmylation and tRNA thiolation in yeast. *Microb Cell.* 2016; 3:554–564. [PubMed: 28357324]
- Jüdes A, Ebert F, Bär C, Thüring KL, Harrer A, Klassen R, Helm M, Stark MJR, Schaffrath R. Urmylation and tRNA thiolation functions of ubiquitin-like Uba4-Urm1 systems are conserved from yeast to man. *FEBS Lett.* 2015; 589:904–909. [PubMed: 25747390]
- Kainth P, Sassi HE, Peña-Castillo L, Chua G, Hughes TR, Andrews B. Comprehensive genetic analysis of transcription factor pathways using a dual reporter gene system in budding yeast. *Methods.* 2009; 48:258–264. [PubMed: 19269327]
- Karim AS, Curran KA, Alper HS. Characterization of plasmid burden and copy number in *Saccharomyces cerevisiae* for optimization of metabolic engineering applications. *FEMS Yeast Research.* 2013; 13:107–116. [PubMed: 23107142]
- Kayikci Ö, Nielsen J. Glucose repression in *Saccharomyces cerevisiae*. *FEMS Yeast Research.* 2015; 15:fov068–fov068. [PubMed: 26205245]
- Kemmeren P, Sameith K, van de Pasch LAL, Benschop JJ, Lenstra TL, Margaritis T, O’Duibhir E, Apweiler E, van Wageningen S, Ko CW, et al. Large-Scale Genetic Perturbations Reveal Regulatory Networks and an Abundance of Gene-Specific Repressors. *Cell.* 2014; 157:740–752. [PubMed: 24766815]
- Khmelniskii A, Blaszczyk E, Pantazopoulou M, Fischer B, Omnis DJ, Le Dez G, Brossard A, Gunnarsson A, Barry JD, Meurer M, et al. Protein quality control at the inner nuclear membrane. *Nature.* 2014; 516:410–413. [PubMed: 25519137]

- Khmelniskii A, Keller PJ, Bartosik A, Meurer M, Barry JD, Mardin BR, Kaufmann A, Trautmann S, Wachsmuth M, Pereira G, et al. Tandem fluorescent protein timers for in vivo analysis of protein dynamics. *Nat Biotechnol.* 2012; 30:708–714. [PubMed: 22729030]
- Kim DU, Hayles J, Kim D, Wood V, Park HO, Won M, Yoo HS, Duhig T, Nam M, Palmer G, et al. Analysis of a genome-wide set of gene deletions in the fission yeast *Schizosaccharomyces pombe*. *Nat Biotechnol.* 2010; 28:617–623. [PubMed: 20473289]
- Kirchner S, Ignatova Z. Emerging roles of tRNA in adaptive translation, signalling dynamics and disease. *Nat Rev Genet.* 2014; 16:98–112. [PubMed: 25534324]
- Klassen R, Ciftci A, Funk J, Bruch A, Butter F, Schaffrath R. tRNA anticodon loop modifications ensure protein homeostasis and cell morphogenesis in yeast. *Nucleic Acids Res.* 2016; 44:10946–10959. [PubMed: 27496282]
- Kramer MH, Farré JC, Mitra K, Yu MK, Ono K, Demchak B, Licon K, Flagg M, Balakrishnan R, Cherry JM, et al. Active Interaction Mapping Reveals the Hierarchical Organization of Autophagy. *Mol Cell.* 2017; 65:761–774.e765. [PubMed: 28132844]
- Lee AY, St Onge RP, Proctor MJ, Wallace IM, Nile AH, Spagnuolo PA, Jitkova Y, Gronda M, Wu Y, Kim MK, et al. Mapping the Cellular Response to Small Molecules Using Chemogenomic Fitness Signatures. *Science.* 2014; 344:208–211. [PubMed: 24723613]
- Lenstra TL, Benschop JJ, Kim T, Schulze JM, Brabers NACH, Margaritis T, van de Pasch LAL, van Heesch SAAC, Brok MO, Koerkamp MJAG, et al. The Specificity and Topology of Chromatin Interaction Pathways in Yeast. *Mol Cell.* 2011; 42:536–549. [PubMed: 21596317]
- Lim WK, Ong CK, Tan J, Thike AA, Ng CCY, Rajasegaran V, Myint SS, Nagarajan S, Nasir NDM, McPherson JR, et al. Exome sequencing identifies highly recurrent MED12 somatic mutations in breast fibroadenoma. *Nat Genet.* 2014; 46:877–880. [PubMed: 25038752]
- Mülleider M, Calvani E, Alam MT, Wang RK, Eckerstorfer F, Zelezniak A, Ralser M. Functional Metabolomics Describes the Yeast Biosynthetic Regulome. *Cell.* 2016; 167:553–565.e12. [PubMed: 27693354]
- Neal S, Jaeger PA, Duttke S, Benner C, Glass C, Ideker T, Hampton RY. The Dfm1 derlin is required for ERAD retrotranslocation of integral membrane proteins. *Mol Cell.* 2018 (in press).
- Nedialkova DD, Leidel SA. Optimization of Codon Translation Rates via tRNA Modifications Maintains Proteome Integrity. *Cell.* 2015; 161:1606–1618. [PubMed: 26052047]
- Ng CCY, Tan J, Ong CK, Lim WK, Rajasegaran V, Nasir NDM, Lim JCT, Thike AA, Salahuddin SA, Iqbal J, et al. MED12 is frequently mutated in breast phyllodes tumours: a study of 112 cases. *J Clin Pathol.* 2015; 68:685–691. [PubMed: 26018969]
- Petrenko N, Jin Y, Wong KH, Struhl K. Mediator Undergoes a Compositional Change during Transcriptional Activation. *Mol Cell.* 2016; 64:443–454. [PubMed: 27773675]
- Plaschka C, Larivière L, Wenzel L, Seizl M, Hemann M, Tegunov D, Petrotchenko EV, Borchers CH, Baumeister W, Herzog F, et al. Architecture of the RNA polymerase II–Mediator core initiation complex. *Nature.* 2015; 518:376–380. [PubMed: 25652824]
- Plempner RK, Bohmler S, Bordallo J, Sommer T, Wolf DH. Mutant analysis links the translocon and BiP to retrograde protein transport for ER degradation. *Nature.* 1997; 388:891–895. [PubMed: 9278052]
- Prasad R, Kawaguchi S, Ng DTW. A Nucleus-based Quality Control Mechanism for Cytosolic Proteins. *Mol Biol Cell.* 2010; 21:2117–2127. [PubMed: 20462951]
- Prather DM, Larschan E, Winston F. Evidence that the Elongation Factor TFIIS Plays a Role in Transcription Initiation at GAL1 in *Saccharomyces cerevisiae*. *Mol Cell Biol.* 2005; 25:2650–2659. [PubMed: 15767671]
- Sassi HE, Bastajian N, Kainth P, Andrews BJ. Reporter-based synthetic genetic array analysis: a functional genomics approach for investigating the cell cycle in *Saccharomyces cerevisiae*. *Methods Mol Biol.* 2009; 548:55–73. [PubMed: 19521819]
- Schuldiner M, Collins SR, Thompson NJ, Denic V, Bhamidipati A, Punna T, Ihmels J, Andrews B, Boone C, Greenblatt JF, et al. Exploration of the Function and Organization of the Yeast Early Secretory Pathway through an Epistatic Miniarray Profile. *Cell.* 2005; 123:507–519. [PubMed: 16269340]

- Schwarzmueller T, Ma B, Hiller E, Istel F, Tscherner M, Brunke S, Ames L, Firon A, Green B, Cabral V, et al. Systematic Phenotyping of a Large-Scale *Candida glabrata* Deletion Collection Reveals Novel Antifungal Tolerance Genes. *PLoS Pathog.* 2014; 10:e1004211–e1004219. [PubMed: 24945925]
- Siraj AK, Masoodi T, Bu R, Pratheeshkumar P, Al-Sanea N, Ashari LH, Abduljabbar A, Alhomoud S, Al-Dayel F, Alkuraya FS, et al. MED12 is recurrently mutated in Middle Eastern colorectal cancer. *Gut* gutjnl–2016. 2017
- Srivasa R, Costelloe T, Carvunis AR, Sarkar S, Malta E, Sun SM, Pool M, Licon K, van Welsem T, van Leeuwen F, et al. A UV-Induced Genetic Network Links the RSC Complex to Nucleotide Excision Repair and Shows Dose-Dependent Rewiring. *Cell Reports.* 2013; 5:1714–1724. [PubMed: 24360959]
- Stolz, A., Wolf, DH. Ubiquitin Family Modifiers and the Proteasome. Humana Press; 2012. Use of CPY\* and Its Derivatives to Study Protein Quality Control in Various Cell Compartments. The Gene Ontology Consortium. Gene Ontology Consortium: going forward. *Nucleic Acids Res.* 2015; 43:D1049–D1056. [PubMed: 25428369]
- Teng X, Dayhoff-Brannigan M, Cheng WC, Gilbert CE, Sing CN, Diny NL, Wheelan SJ, Dunham MJ, Boeke JD, Pineda FJ, Hardwick JM. Genome-wide Consequences of Deleting Any Single Gene. *Mol Cell.* 2013; 52:485–494. [PubMed: 24211263]
- Tkach JM, Yimit A, Lee AY, Riffle M, Costanzo M, Jaschob D, Hendry JA, Ou J, Moffat J, Boone C, et al. *Nat Cell Biol.* 2012; 14:966–976. [PubMed: 22842922]
- Tong W, Kulaeva OI, Clark DJ, Lutter LC. Topological Analysis of Plasmid Chromatin from Yeast and Mammalian Cells. *J Mol Biol.* 2006; 361:813–822. [PubMed: 16890953]
- Traven A, Jelicic B, Sopta M. Yeast Gal4: a transcriptional paradigm revisited. *EMBO Reports.* 2006; 7:496–499. [PubMed: 16670683]
- van de Peppel J, Kettelarij N, van Bakel H, Kockelkorn TTJP, van Leenen D, Holstege FCP. Mediator Expression Profiling Epistasis Reveals a Signal Transduction Pathway with Antagonistic Submodules and Highly Specific Downstream Targets. *Mol Cell.* 2005; 19:511–522. [PubMed: 16109375]
- Vizeacoumar FJ, van Dyk N, Vizeacoumar FS, Cheung V, Li J, Sydorsky Y, Case N, Li Z, Datti A, Nislow C, et al. Integrating high-throughput genetic interaction mapping and high-content screening to explore yeast spindle morphogenesis. *J Cell Biol.* 2010; 188:69–81. [PubMed: 20065090]
- Wang H, Shen Q, Ye LH, Ye J. MED12 mutations in human diseases. *Protein Cell.* 2013; 4:643–646. [PubMed: 23836153]
- Willingham S. Yeast Genes That Enhance the Toxicity of a Mutant Huntingtin Fragment or alpha-Synuclein. *Science.* 2003; 302:1769–1772. [PubMed: 14657499]
- Winzeler EA, Shoemaker DD, Astromoff A, Liang H, Anderson K, André B, Bangham R, Benito R, Boeke JD, Bussey H, et al. Functional Characterization of the *S. cerevisiae* Genome by Gene Deletion and Parallel Analysis. *Science.* 1999; 285:901–906. [PubMed: 10436161]
- Wolff S, Weissman JS, Dillin A. Differential Scales of Protein Quality Control. *Cell.* 2014; 157:52–64. [PubMed: 24679526]
- Zhu X, Wirén M, Sinha I, Rasmussen NN, Linder T, Holmberg S, Ekwall K, Gustafsson CM. Genome-Wide Occupancy Profile of Mediator and the Srb8-11 Module Reveals Interactions with Coding Regions. *Mol Cell.* 2006; 22:169–178. [PubMed: 16630887]



**HIGHLIGHTS**

- New mutant library and screening technology for high-content phenotype data in yeast
- Enables phenotype-specific exploration of gene, pathway, and condition relationships
- Expression reporter: Mediator complex is necessary to maintain glucose repression
- Degradation reporter: U<sub>34</sub> tRNA modifications play an important role in protein folding

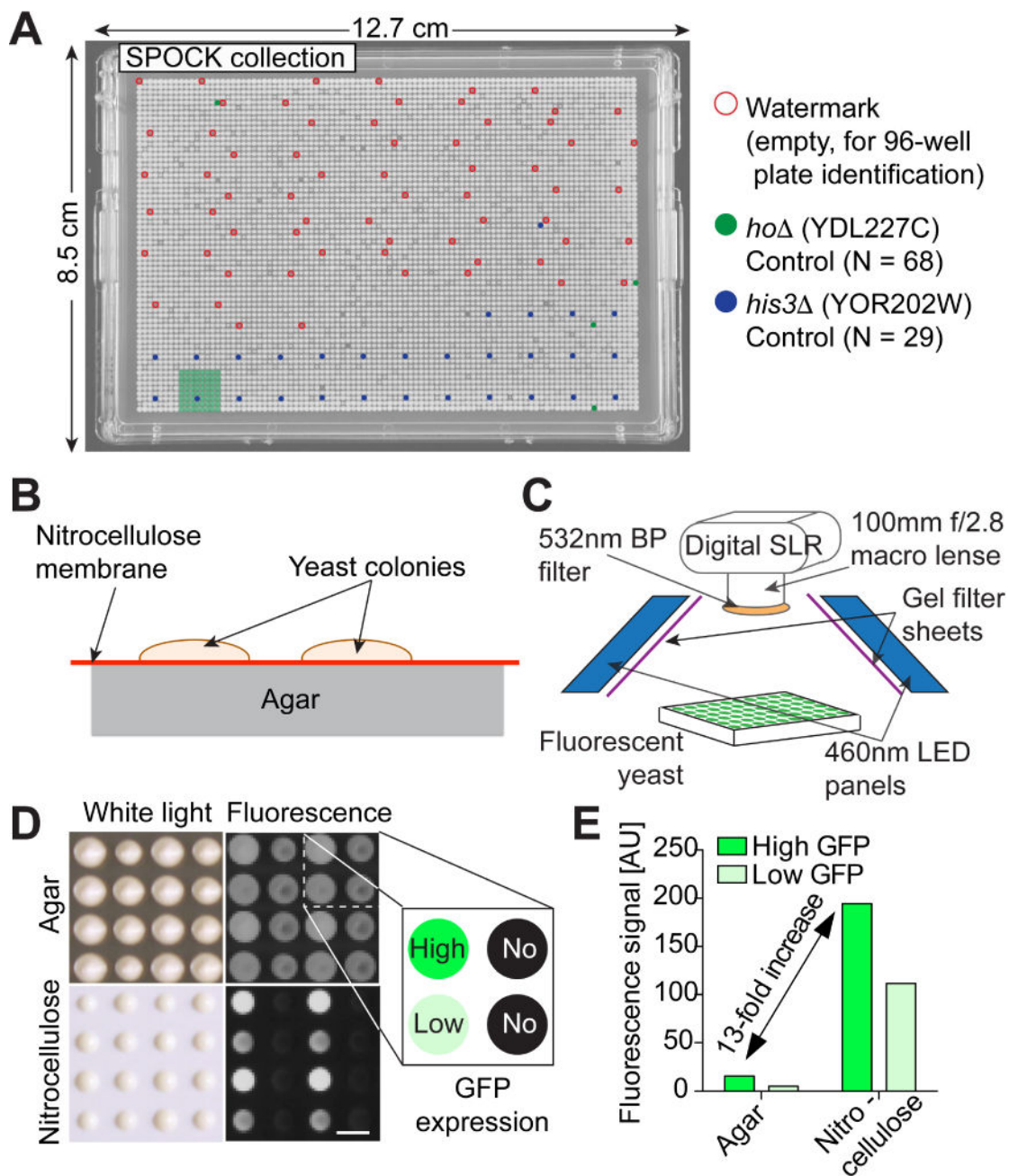


**Figure 1. Systematic gene-to-phenotype arrays (SGPA)**

(A) Overview of SPOCK covering >95% of all yeast ORFs. (B) For SGPA, yeast colonies grow on nitrocellulose instead of agar directly. (C) Imaging setup for the fluorescence screening. (D) Comparison of high, low, and no-GFP test strains grown on traditional agar plates (top row) and on nitrocellulose (bottom row); scale bar 2mm. (E) Thirteen-fold increase in signal due to growth on nitrocellulose (signal minus no-GFP background intensity, mean of N=384 for each, error bars too small to display).

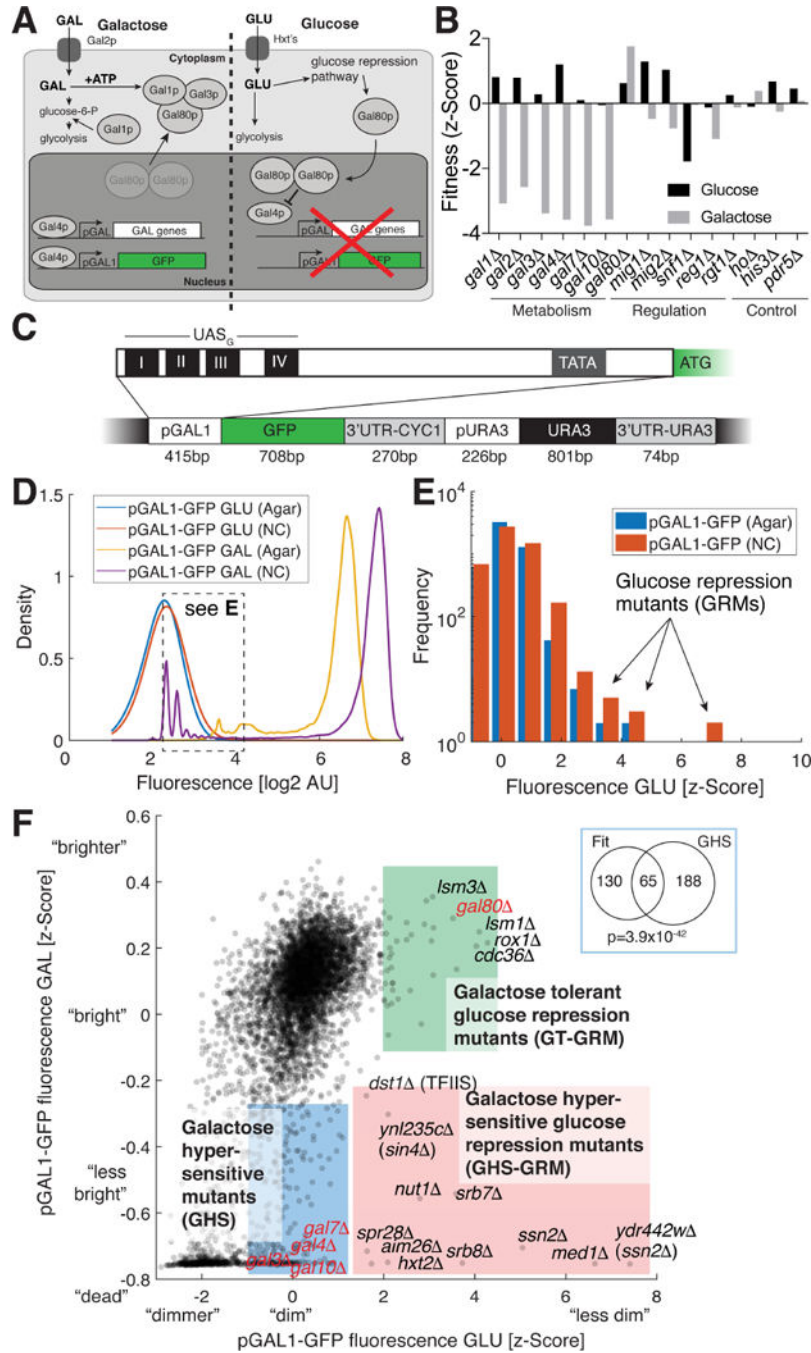


**Figure 2. Study of glucose repression genes by SGPA**

(A) Overview of the galactose and glucose pathways; pGAL1-GFP represents our artificial promoter activity sensor on a 2 $\mu$  plasmid. (B) Analysis of fitness defects in galactose pathway mutant strains grown with glucose (black bars) or galactose (gray bars) as sole carbon source (mean of N=5). (C) Schematic of the reporter cassette: the pGAL1 contains four Upstream Activating Sequences for Gal4p transcription factor binding (UAS<sub>G</sub>) and the *GAL1* TATA box. It also contains a selectable auxotrophic marker (*URA3*) under a separate promoter, as well as termination sequences (3' UTR). (D) Fluorescence distribution for

colonies grown under glucose on agar (blue) or nitrocellulose (red), and colonies grown under galactose (yellow, purple). **(E)** Distribution of the z-Scored colonies fluorescence values for the repressed glucose conditions. **(F)** Scatter graph showing the pGAL1-GFP fluorescence values under repressed glucose *versus* induced galactose conditions. Values around zero represent colonies with close-to-population-average intensities under the respective conditions. See text for mutant classifications; selected mutants are named for clarity; red labels are examples of typical, known galactose pathway mutants. Inset shows overlap in hits between a classical, fitness based assay of glucose-galactose switch and the GHS mutants.

Author Manuscript

Author Manuscript

Author Manuscript

Author Manuscript

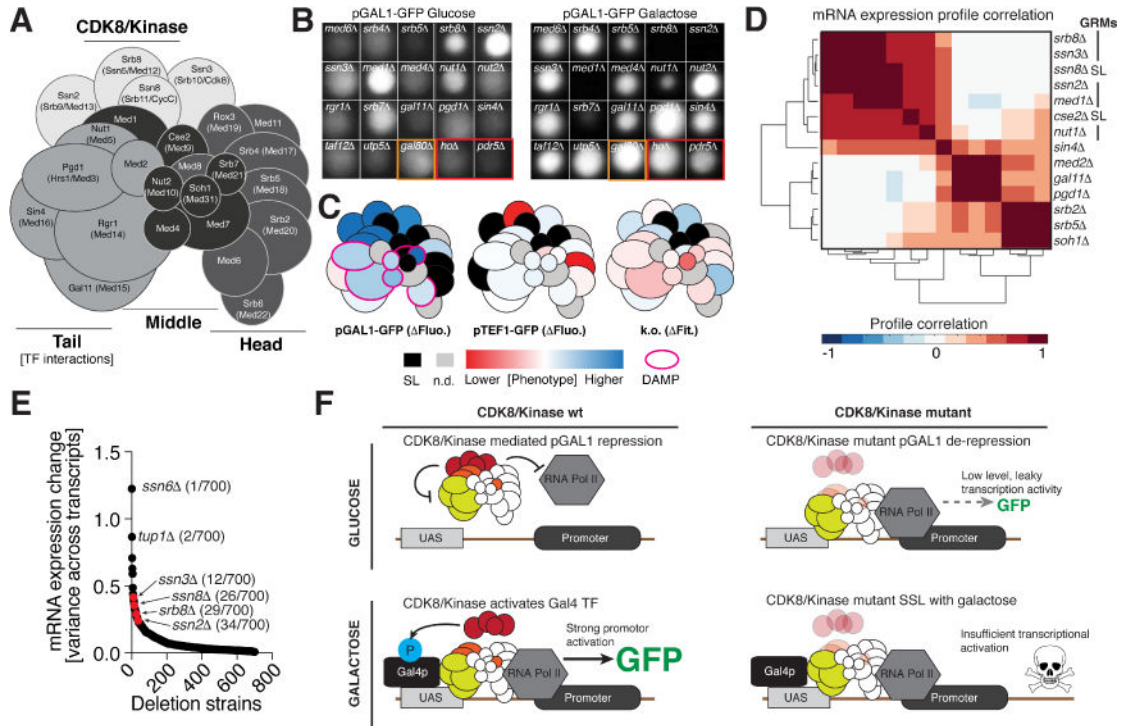


**Figure 3. A role for Mediator CDK8/kinase module in pGAL1 repression and activation**  
**(A)** Schematic of the Mediator complex and the four functional modules (Tail, CDK8/Kinase, Middle, Head). **(B)** Representative examples of Mediator mutant colonies, compared to the most potent mutants from the SAGA complex (*taf2* and *utp5*); *gal80* as positive control (orange box), and *ho* and *his3* as negative controls (red box, box size ~2mm.). *Note: The exposure of the glucose mutants has been enhanced (linearly for all mutants) to make the otherwise very faint colonies visible for comparison to galactose grown colonies.* **(C)** Mapping to the Mediator complex of the corresponding genotype-phenotype changes between glucose and galactose as carbon source for pGAL1-GFP fluorescence, pTEF1-GFP fluorescence (negative control), and colony fitness. Black subunits were lethal in the respective screen, gray subunits were not in SPOCK, pink outline represents DAMP mutants for essential genes. **(D)** Unsupervised clustering of expression profiles for mediator mutants across ~3000 transcripts under glucose. GRM bar indicates strongest GRM mutants. **(E)** Ranked variance for 700 gene deletions across ~3000 transcripts. Red dots indicate CDK8/Kinase mutant strains, value in brackets represent the rank. **(F)** Proposed model of the bi-modal role of the CDK8/Kinase module of Mediator in tight repression under glucose and strong induction under galactose conditions (left side) and the effects of CDK8/Kinase module mutants (right side, see text for details).



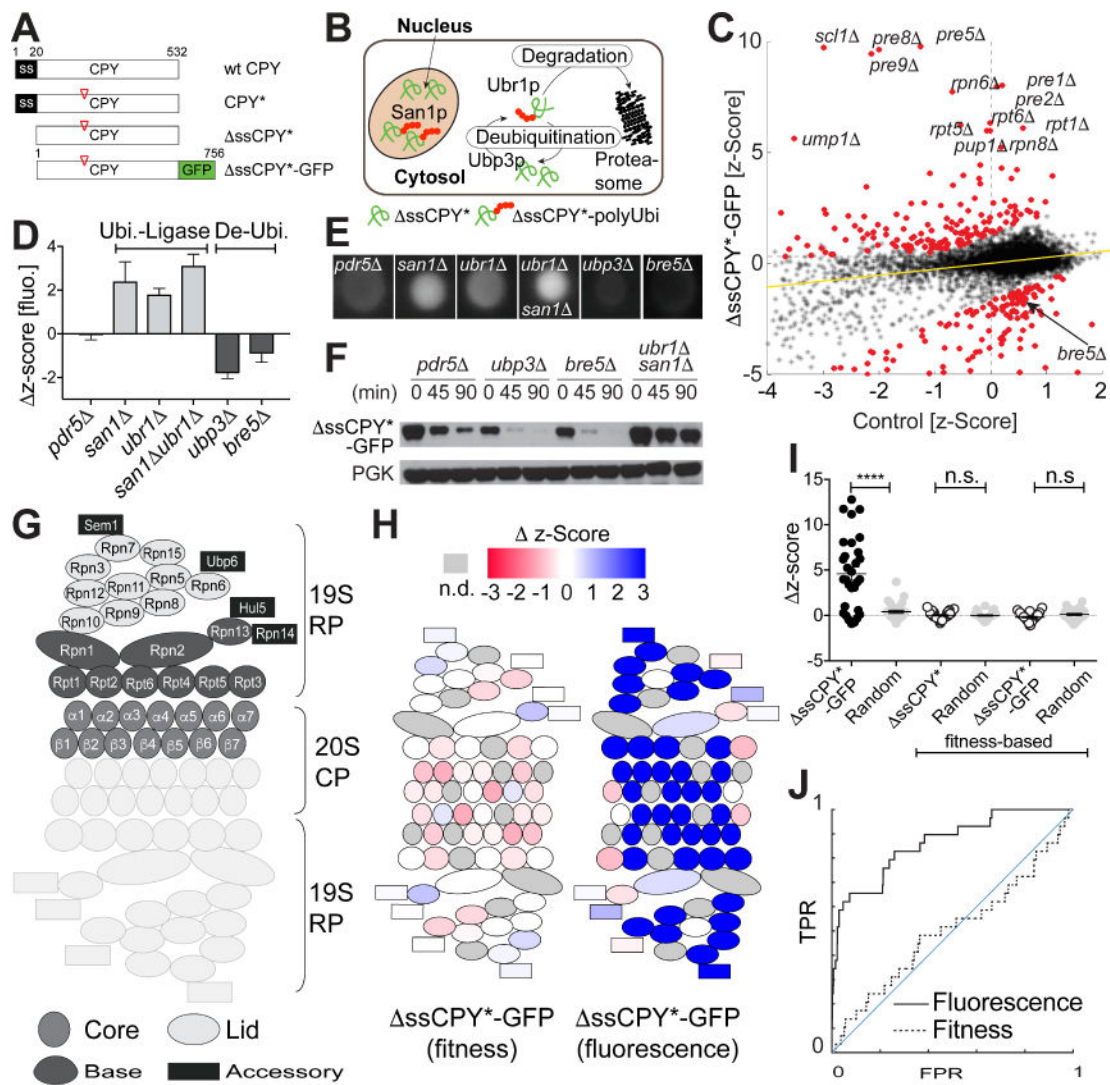


**Figure 4. Study of protein quality control genes by SGPA**

(A) Overview of Carboxypeptidase Y (CPY) mutants (red triangle denoted point mutation, numbers indicate amino acid position). (B) Schematic representation of  $\Delta$ ssCPY\*-GFP localization, ubiquitination, deubiquitination, and proteasomal degradation. (C) Mutants of genes involved in PQC (red) were identified based on the differential relative fluorescence ( $\Delta$  z-score) between each mutant expressing either  $\Delta$ ssCPY\*-GFP or GFP alone (yellow line, least squares fit). Mutants of genes normally promoting degradation are above, those of genes normally slowing degradation are below the yellow line. (D) SGPA  $\Delta$  z-scores of known ubiquitinating and deubiquitinating enzymes are shown along with those of BRE5, a previously unappreciated PQC component. (E) Representative colonies for the mutants in (c), box size ~2mm. (F) Western-blot analysis of  $\Delta$ ssCPY\*-GFP degradation following cycloheximide treatment (*pdr5 $\Delta$*  serves as 'wildtype' control). (G) Schematic of the 30 subcomponents of the proteasome complex. (H) Fitness (left) and SGPA fluorescence (right) scores for the 30 proteasome-mutant  $\Delta$ ssCPY\*-GFP strains. (I) Comparison between SGPA fluorescence (black) and fitness scores (white) for the 30 proteasome mutants, with and



without the GFP fusion or equally sized sets of random control genes (grey; MWU test, \*\*\*\* $p < 0.0001$ , n.s. not significant). (J) ROC curve for the successful identification of the 30 proteasome mutants using SGPA versus fitness scores (TPR, true positive rate; FPR, false positive rate).

Author Manuscript

Author Manuscript

Author Manuscript

Author Manuscript

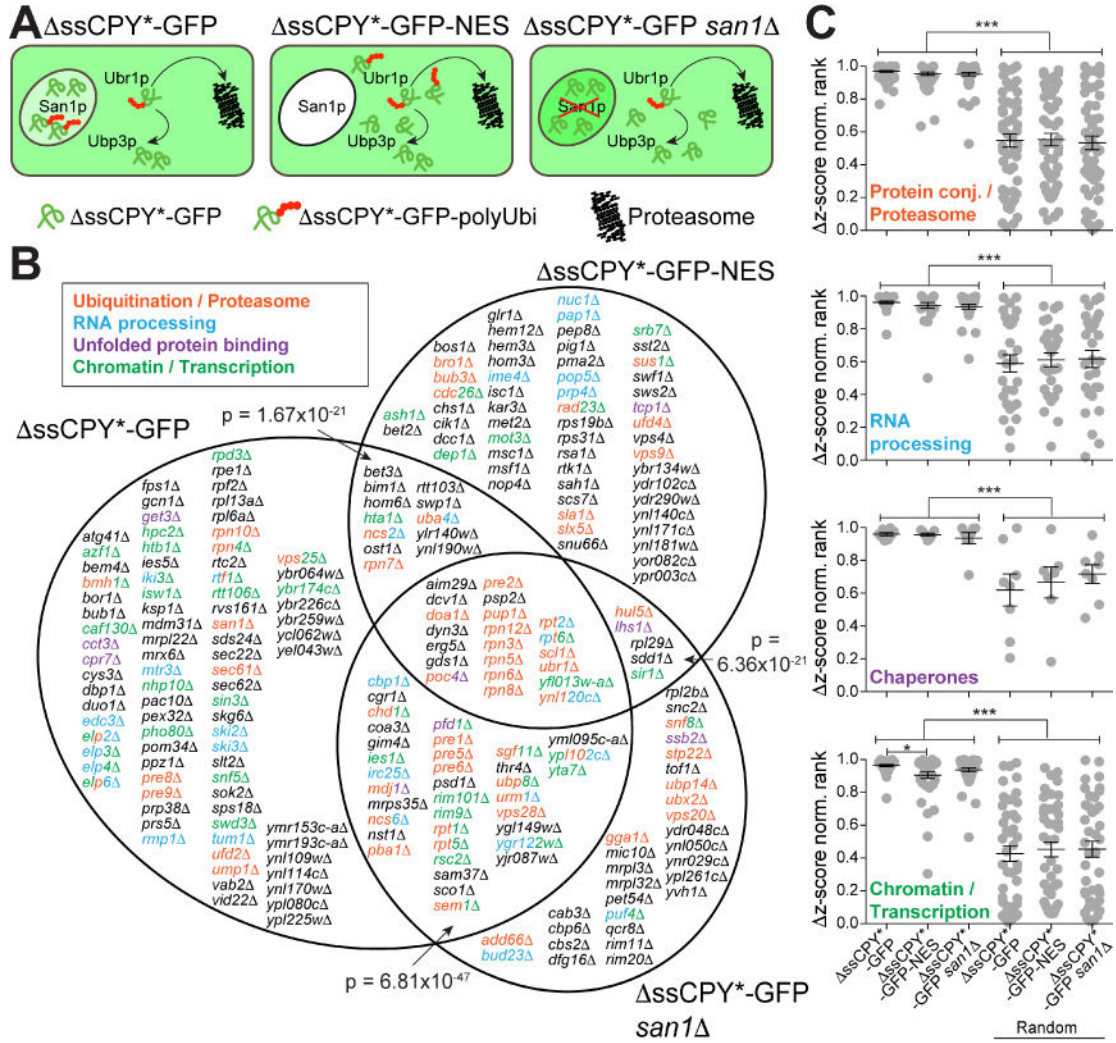


**Figure 5. Identifying genes important for PQC**

(A) Schematic of the three sequential screens using different localization of the main ssCPY\* expression and degradation (see text for details, (Heck et al., 2010; Prasad et al., 2010)). (B) Venn-diagram for the 244 genes with elevated fluorescence identified in the three independent screens. P-values indicate binary overlap between sets, including the triple hits from the center (Fisher’s exact test). Colors indicate high-level functional annotation of enriched groups (see Figure S5). (C) Ranked (1=highest, 0=lowest score) differential fluorescence scores between hits from the three screens, binned into the four main functional classes, and similarly sized random control groups (ANOVA followed by Tukey’s comparison).

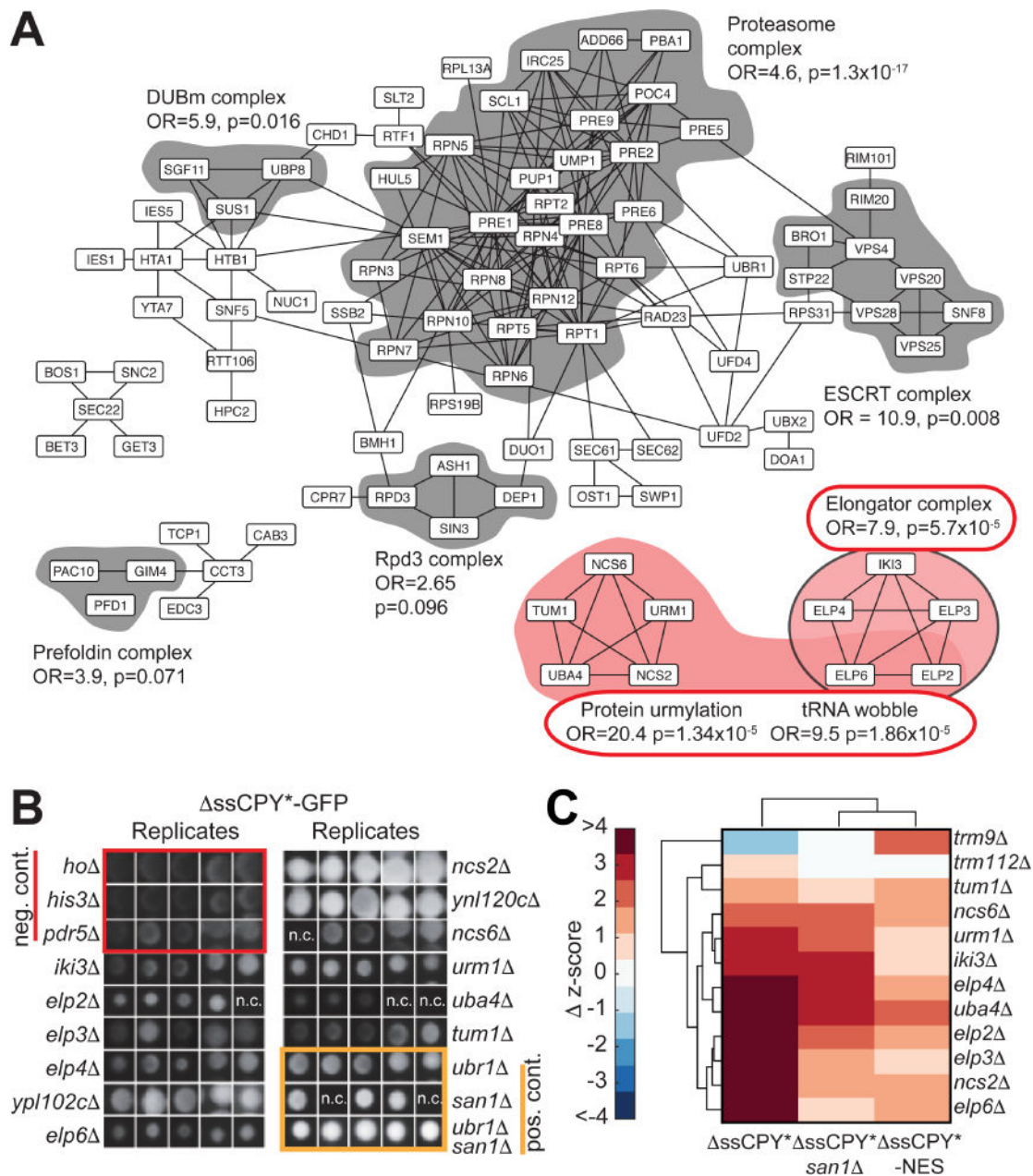


**Figure 6. Functional and protein complex enrichment reveals a role for tRNA modification in the process of protein quality control**

(A) Overlay of the gene hits on a protein-protein interaction network (from BioGRID).

Complexes with  $p < 0.1$  (full GO enrichment, BH corrected) are outlined, singlet genes and genes pairs are removed for clarity. Networks highlighted in red relate to  $U_{34}$  tRNA modification and protein urmylation. (B) Colony view of the  $\Delta$ ssCPY\*-GFP mutants relevant to tRNA modification (n.c. = no colony growth). (C) Clustering of SGPA scores of the tRNA modification deficient mutants.

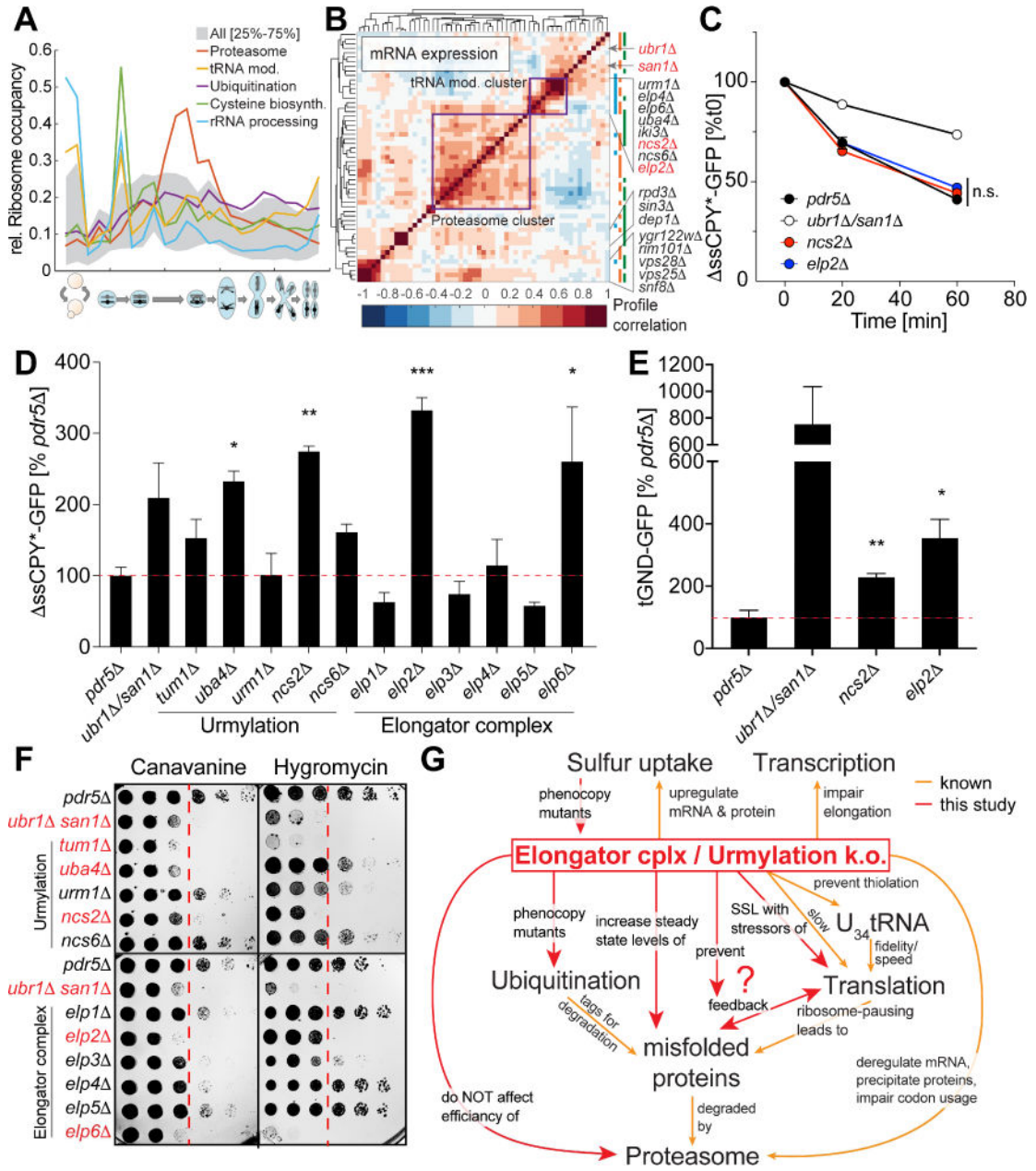


**Figure 7. Mechanistic impact of U<sub>34</sub> tRNA modification deficiency**

(A) Expression analysis of protein degradation or tRNA modification genes across yeast cell cycle stages by ribosome profiling. (B) mRNA expression changes induced by selected gene deletions identified by SGPA as important to protein quality control. Right hand color stripes indicate superclass annotations (blue = RNA processing, orange = proteasome, green = chromatin/histones). (C) FACS pulse-chase time course of  $\Delta$ ssCPY\*-GFP degradation (*pdr5* serves as ‘wildtype’ control, N=4 for each mutant and time point). (D) Steady-state concentration of  $\Delta$ ssCPY\*-GFP relative to *pdr5* GFP-only values (N=3 for each mutant, FACS). (E) Steady-state concentration of tGND-GFP relative to *pdr5* control (N=3 for each mutant, FACS). (F) Synthetic lethality screen with translation inhibitors (Can 0.25

µg/ml, Hyg 62.00 µg/ml). Red line indicates half-way point for control strains without growth defects. Strains that are qualitatively considered synthetic sick/lethal are indicated in red. **(G)** Schematic of the proposed effects of U<sub>34</sub> tRNA modification deficiency on protein quality control.

Author Manuscript

Author Manuscript

Author Manuscript

Author Manuscript